Low Cost Watermarking Based on a Human Visual Model

J.F. Delaigle, C. De Vleeschouwer [1], F. Goffin,
B. Macq, J.-J. Quisquater
Laboratoire de Télécommunications et Télédétection
Université catholique de Louvain
Bâtiment Stévin - 2, place du Levant
B-1348 Louvain-la-Neuve
Tel.: +32 10 47.41.05 - Fax.: +32 10 47.20.89
E-mail: {delaigle, devlees}@tele.ucl.ac.be

Abstract. This paper presents an additive watermarking technique for grey scale pictures, which can be extended to video sequences. It consists of embedding secretly a copyright information (a binary code) in the picture without degrading its quality. Those bits are encoded through the phase of Maximal Length Sequences (MLS). MLS are sequences having good correlation properties, which means that the result of the autocorrelation is far greater than crosscorrelations, i.e. correlations made with shifted version of this sequence. This embedding is performed line by line going from the top to the bottom of the picture as the objective was to implement a low cost and real time embedding method able to work for common video equipments. The very embedding process is underlain by a masking criterion that guarantees the invisibility of the watermark. This perceptive criterion, deduced from physiological and psychophysic studies, has already proved its efficiency [DDVB96]. It is combined with an edge and texture discrimination to determine the embedding level of the MLS, whose bits are actually spread over 32 by 8 pixel squares. Eventually, some preliminary results are presented, which analyze the efficacy of the decoding as well as the resistance of the watermark towards compression and robustness against malevolent treatments.

1 Introduction

Copyrights offer protection for the contents of the exchanges which take place on the networks. As the Information Society evolves, it is expected that more and more works and other protected material will be carried by the Superhighway. It is clear that with the increasing of digitization, classical legal protection is not sufficient but the development of technical protection tools will be the key to the realization of the Information Society. Indeed the acceptance of new digital audiovisual services depends on whether suitable techniques for the protection of the work providers' interests are available [Kah94].

[1]Research of C. De Vleeschouwer is supported by a grant of the Belgian F.N.R.S. - Alcatel Bell.

Actually, the very nature of digital media threatens its own viability. First the replication of digital works is very easy and, what is more dangerous, really perfect. The copy is identical to the original content. The ease of transmission and multiple uses is very worrying, too. Once a single unauthorized copy has been made, it is instantaneously accessible to anyone who wants it, without any control of the owner of the original content. Eventually the plasticity of digital media is a great menace. Any malevolent user *(a pirate)* can modify an image at will. Such manipulations are really easy with the existing image processing tools and put many copyright protection methods at risk.

Fortunately, digitization of audiovisual contents offers in counter part new possibilities for the development of copyright protection techniques. Watermarking is one of these. The principle of the watermarking is the robust embedding of a copyright information (e.g. time and date, Copyright Identifier etc.) in a content. This content may be a text [MT94] [BSLO94], the audio [BGM95], but most of the time watermarking is applied to still or moving images. Precisely this paper is focusing on still images watermarking.

Many labs and companies have already developed their own watermarking techniques for still images. Most of them directly work on the luminance with or without any considerations about the quality of the watermarked image [BQM95, Car95]. It is also interesting to consider the image content as a channel that can convey a certain quantity of information. Different techniques use this approach by means of the spread-spectrum theory to embed a copyright code [CKLS95]. Finally, other authors apply the watermarking not on the picture itself but on some of its characteristics, like DCT coefficient [KZ95], fractal coefficients or motion estimation vectors, high resolution coefficient in case of multiresolution encoding [MQ94].

These techniques give different results with different quality levels, but all have in common that they have to realize a good trade-off between the robustness of the watermarking, the quality of the watermarked picture and the computational cost. However, very few of them really analyze the quality of the resulting image. Only one previously presented algorithm really uses a human visual model to guarantee the invisibility of the embedding [DDVB96]. The method presented in this paper is a derivative of the precited method. It tends to improve its computational cost and to permit the embedding of more bits in the image. An other important point is the fact that the retrieval of the embedded copyright information does not require the use of the original picture, so that no human intervention is needed for the decoding of the watermark. This advantage is essential in case of the utilization of the watermarking for an automated monitoring of copyrighted works.

2 Perceptive Model

Given that the goal of a watermarking technique is to embed some information in a content. In the case of picture content, the watermark must be hidden (*masked*) by the picture it is inlayed in. The watermarking method presented in this paper precisely refers to a masking criterion deduced from physiological and psychophysic studies [Com95].

2.1 Eye Functioning and Masking Concept

It is now admitted that the retina of the eye splits the visual stimulus composing an image in several components. These components circulate from the eye to the cortex by different tuned channels, one channel being tuned to one component. The characteristics of one component are:

- the locations in the visual field (in the image).
- the spatial frequency (in the Fourier domain: the amplitude in polar coordinates).
- the orientations (in the Fourier domain: the phase in polar coordinates)

One perceptive channel can only be excited by one component of a signal whose characteristics are tuned to its. Components that have different characteristics are independent. Moreover, according to perceptive model of human vision [WOT86], signals that have same (near) components take the same channels from the eye to the cortex. It appears that such signals interact and are submitted to non-linear effects. The ***masking*** is one of those effects. It occurs when the ***detection threshold***, i.e. the minimum level below which a signal can not be seen, is increased because of the presence of another signal. In other words, the masking occurs when a signal can not be seen because of another with near characteristics and at a higher level.

2.2 The Masking Model

With the object of modelizing the masking phenomenon, tests have been made on monochromatic signals, also called ***gratings***, i.e. signals of one single frequency and one orientation (f_0, θ_0). It appeared that the eye is sensitive to the contrast of those gratings. L being the luminance, this contrast is defined by:

$$C = \frac{2(Lmax - Lmin)}{Lmax + Lmin} \tag{1}$$

It is possible to determine experimentally the detection threshold of one signal of contrast C_s with respect to the contrast C_m of the masking signal. That threshold can be expressed for gratings featured by (f_0, θ_0) as:

$$C_{s_{(f_0, \theta_0)}}(C_m) = max[C_0, C_0(\frac{C_m}{C_0})^{\epsilon}] \tag{2}$$

where ϵ (the slope) depends on (f_0, θ_0), typically, $0.6 \leq \epsilon \leq 1.1$.

It is possible to extend that expression to introduce frequency and orientation dependence. So, the general expression of the detection threshold becomes:

$$C_s(C_m;f;\theta) = C_0 + k_{(f_0;\theta_0)}(f;\theta)[C_{s_{(f_0,\theta_0)}}(C_m) - C_0] \tag{3}$$

where:

$$k_{(f_0;\theta_0)}(f;\theta) = exp[-(\frac{log^2(\frac{f}{f_0})}{F^2(f_0)} + \frac{(\theta-\theta_0)^2}{\Theta^2(f_0)}] \tag{4}$$

In this expression, f_0 and θ_0 are relevant to the masking signal, f and θ are relevant to the masked signal, $F(f_0)$ and $\Theta(f_0)$ are parameters that represent the spreading of the Gaussian function, C_0 is often negligible. The spread of the gaussian function depends upon the frequency f_0: for frequency, typical bandwidth at half response are 2,5 octaves at 1 c/d and 1,5 octaves at 16 c/d with a linear decrease between both frequencies [WMP83]; for orientation, half bandwidth at half response depends on f_0 and it takes typical values like 30 degrees at 1 c/d and 15 degrees at 16 c/d [WP84]. According to this expression, the frequency dependence of the detection threshold has a Gaussian form. Only near frequency signals can interact. When the frequency of the masking signal (the mask) is far from the one of the signal to mask, the detection threshold is almost equal to C_0.

2.3 The Masking Criterion

It is important to notice that those results concern only gratings signals. To deduce a masking criterion that applies to signals like real images, the preceding masking condition has to be adapted. So, it is necessary to define a new concept able to take the place of the contrast, because the contrast is not define for real images. That new concept [Com95] is the ***local energy***, $E_{(f_0;\theta_0)}(x;y)$. The local energy is defined on narrowband signals centered around one frequency and one orientation. A picture which is a broadband signal is first filtered by Gabor narrowband filters (see equation 5), whose characteristics are tuned to a particular perceptive component and which are near to human perception. **The local energy in this component corresponds to the amplitude of the envelop of the resulting bandpass signal**. In the framework of the analytic representation of signals, i.e. signals are described only by positive frequencies, the local energy is calculated following the scheme presented in this figure:

I(x ,y) → [analytic filters $(f_0;\theta_0)$] → [$|\cdot|^2$] → $E_{(f_0;\theta_0)}(x;y)$

Having introduced this local energy concept, **the masking criterion** can be defined: "Strictly, a noise is masked by a mask
if $\forall$ *pixel* $(x;y)$ and $\forall(f_0;\theta_0)$, $E_{mask;(f_0;\theta_0)}(x;y) \geq E_{noise;(f_0;\theta_0)}(x;y)$".

2.4 Perceptive Filter in the Horizontal Direction

In Fourier space, analytic filters used to extract the local energy are defined by:

$$G_{(f_0,\theta_0)}(f,\theta) = exp[-(\frac{log^2(\frac{f}{f_0})}{F^2(f_0)} + \frac{(\theta-\theta_0)^2}{\Theta^2(f_0)}] \quad (5)$$

In the following, only filters in the horizontal orientation will be useful (i.e. $\theta_0 = 0$). If u and v designate horizontal and vertical frequencies (i.e. corresponding to x and y directions), if u_0 is the central horizontal frequency and if the filter is narrow band according to u frequency, appropriate Gabor analytic filters can be approximated by the following separable filters:

$$G_{u_0}(u,v) = exp[-(\frac{log^2(\frac{u}{u_0})}{F^2(u_0)})].exp[-(\frac{v}{u_0.sin(\Theta(u_0))})^2] = G_{1,u_0}(u).G_{2,u_0}(v) \quad (6)$$

Making the common hypothesis that the observer is located at a distance equal to 6 times the picture height, *cycles/degree* frequencies can be converted into normalized frequencies according to the sampling frequency. Indeed, N being the number of column of the picture (i.e. the width of the picture),

$$f_{norm}(\frac{cycles/screen}{Nbr\ of\ samples\ on\ screen}) = \frac{f(cycles/degree) \times 9.53(degrees/screen)}{N(Number\ of\ samples\ on\ screen)} \quad (7)$$

As the sampling rate is the same in both horizontal and vertical directions, the normalization factor $\frac{9.53}{N}$ is also valid to convert *cycles/degree* horizontal frequencies into normalized frequencies. So, according to the above considerations about the bandwidth of the filter defined by equation 4, $F(u_0)$ and $\Theta(u_0)$ in equation 6, u_0 being a normalized frequency, are defined in term of normalized frequencies as:

$$F(u_0) = \frac{\frac{-1}{15}.(\frac{u_0.N}{9.53}-1)+2.5}{\sqrt{ln(2)}}$$

$$\Theta(u_0) = \frac{31-\frac{u_0.N}{9.53}}{\sqrt{ln(2)}}$$

In the spatial (x,y) domain, the inverse Fourier transform of $G_{u_0}(u,v)$ is $g_{u_0}(x,y) = g_{1_{u_0}}(x).g_{2_{u_0}}(y)$. $g_{1_{u_0}}(x)$ is designed by inversion of the Discrete Fourier Transform (DFT) obtained by sampling $G_{1_{u_0}}(u)$. Tests have shown that 15 samples are sufficient to have a good approximation of the ideal filter. $g_{2_{u_0}}(y)$ can be expressed analytically (as the inverse Fourier transform of a Gaussian function). 9 samples are sufficient to generate a good filter approximation:

$$g_{2,u_0}(y) = \frac{u_0.sin(\Theta(u_0))}{\sqrt{2}}.exp[-(\pi.y.u_0.sin(\Theta(u_0)))^2] \quad (8)$$

3 Information Embedding

3.1 Method Major Features

Looked from the angle of the information theory, watermarking is similar to transmitting a bitstream through a very noisy channel, which is the original picture, under the demanding constraint of watermark invisibility. It is with this aim in view that that the watermark is generated line by line going from the top to the bottom of the image, similarly to the analog TV process. A local examination of the picture content in the horizontal perceptive component is done. This permits to modulate the energy of the signal carrying the bitstream information. The objective is to implement a low computational cost and real time embedding method able to work for common video equipments.

3.1.1 Maximum Length Sequences (MLS): L orthogonal Codewords

The high noise in the transmission channel lead to spread the information bitstream over binary code words. Code words are sequences of 1 and -1 symbols. The decoding of these code words is performed through correlations. This entails the use of orthogonal code words. Moreover, equiprobable sequences symbols are advantageous in order to reduce the effect of the noise on the correlations.

Maximal Length Sequences (MLS) perfectly fulfill these requirements, since MLS sequences are nearly orthogonal to their shifted versions. Crosscorrelations between shifted versions are equal to -1, whereas autocorrelations are equal to the length of the MLS sequence. Moreover, they are also referred to as pseudorandom sequences, because the various statistics associated with the symbols occurrences are close to those associated with coin-toss sequences [SM80]. MLS exist for all integer values n, with a period $L = 2^n - 1$, and can be easily generated by proper connections of feedback paths in an n-stage shift register circuit [Pet].

In the rest of the paper, the L codewords of the L-ary system are thus shifted versions of a particular MLS. n Bits are coded through the phase, i.e. the number of shifts, of a $L = 2^n - 1$ long sequence. The choice of the length L is the result of a trade off. A long sequence permits a more efficient and reliable decoding. On the other hand, making the sequence longer decreases the number of bits encrusted in the image. A good compromise is the use of a 31 symbols long sequence, i.e. $n = 5$. So, as every symbol is spread over 8×32 pixels rectangles (see section 3.1.2, a 512×512picture can support 33 MLS of 5 information bits each, this leads to a total of 165 bits embedded in a 512×512 picture.

3.1.2 Inscription in Perceptive Component

Once the basic information has been coded through the MLS phase, the resulting sequence has to be embedded in the picture. This has to be made in a way that ensures invisibility, undetectability, resistance towards malevolent manipulations and guarantees a correct decoding.

Another paper [DDVB96] has proved the efficacity of masking concepts in order to ensure the invisibility of an additive information in a picture. These masking concepts have been described in section 2. A major feature of the Human Visual System is the fact that the retina of the eye splits the observed picture in components characterized by their location, their spatial frequency, and their orientation. In order to simplify the use of the masking concepts (see section 3.2), it has been decided to excite one single perceptive component at a time. This excited component is of course horizontal, due to the TV-like scanning of the picture. To generate a signal having spectral components around the central frequency of the excited perceptive channel, the MLS modulates a carrier at this frequency. This frequency changes for each MLS embedded in the picture. The choice of the frequenciesis secret in order to make the watermark resistant against piracy, since a malevolent user is not able to remove the watermark from the picture without knowing this secret frequency. **The choice of the possible carriers is limited to the interval of normalized frequencies** [0.1, 0.2]**.** The perceptive model is less valid and less effective for lower frequencies and the image content does not permit to watermark at a sufficient level for higher frequencies. Moreover, higher frequency image features are less visible and can be removed without disturbing the global picture quality. So, a filtering may also remove the watermark.

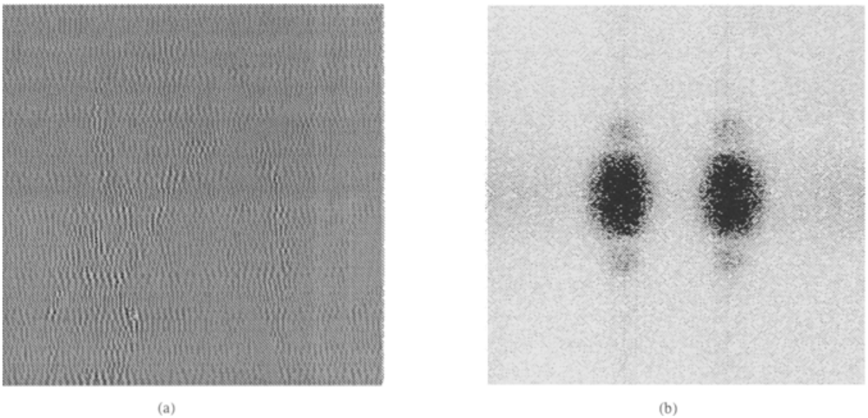

Figure 1: Lena's watermark: (a) spatial domain, (b) Fourier space.

In order to stimulate only one perceptive component (i.e. the horizontal perceptive component), the resulting signal has to be narrow band in both vertical and horizontal directions. This means that each symbol of the MLS must be spread on a few lines and a few columns. In the proposed implementation, each symbol of the MLS corresponds to a 8 pixels high and 32 pixels wide rectangle. Figure 3.1.2(b) presents the spectrum (Fourier transform) of an example of an embedded signal, i.e. the watermark evaluated on the "Lena" picture (see figure 3.2.2(a)). The watermark appears to be spread on neighboring perceptive components. So, ideally the masking criterion should be verified for these perceptive components. Nevertheless, as the major part of the watermark is concentrated in the horizontal component, one may admit that, if the invisibility criterion is verified for this component then the watermark is invisible in the whole picture. This assumption has been corroborated through experiments.

As the inscription is generated on groups of eight lines, during the decoding, each group of eight lines is also considered as a whole. Figure 3.2 illustrates the receiver for this L-ary orthogonal codeword signaling. The center frequency of the band pass filtering and the demodulation frequency are adapted in order to follow the frequency hopping, i.e. the change of the MLS carrier frequency. The knowledge of this frequency hopping is the secret part of the inscription. The synchronization part of the decoder is discussed in section 4.2.2.

3.2 Invisibility Requirement

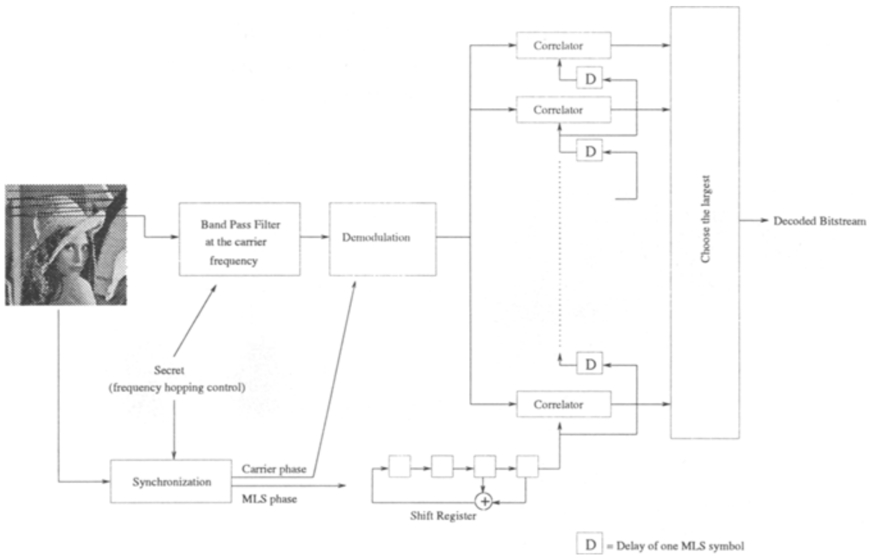

Figure 2: Receiver for L-ary Orthogonal-Codeword Signaling.

This section, describes how to determine the inscription level according to the picture content. A two stages filtering process has been implemented:

- Firstly, a perceptive analytic filter adapted to the frequency of the MLS carrier is used to estimate the masking capabilities of the picture in the studied area and in the perceptive component in which the MLS is embedded.
- Secondly, a high frequency filter detects the main features (i.e. the edges) of the picture and, thanks to a spatial morphological filtering, distinguishes between uniform and textured areas to correct the perceptive model imperfections.

The two results of these filtering processes are then combined to produce an energy level whose square root fixes the local inscription level.

3.2.1 Perceptive Analytic Filtering

The masking criterion (see section 2.3) is strongly simplified when the noise is contained in a single perceptive component. In this case, the noise designates the watermark while the mask corresponds to the original picture. The perceptive component is characterized by the horizontal orientation and by the MLS carrier frequency u_0. So, the noise is perceptively invisible in the mask if $\forall(x,y)$, $E_{mask,u_0}(x,y) \geq E_{noise,u_0}(x,y)$ with E being the local energy defined in section 2.3.

The local energy of the original image is extracted by the analytic filters defined in section 2.4. The local energy of the image formed with the MLS could be extracted in the same way. Nevertheless, due to the small bandwidth of this signal and to the concentration of its spectrum around the central frequency of the perceptive component, it can be assumed that Gabor filtering does not modify the modulated MLS. As a consequence, the local energy can be approximated by the local amplitude of the image formed with the MLS.
So, to satisfy the masking criterion, one has to choose an amplitude $A(x,y)$ for the MLS that is lower than the local energy of the original picture in the perceptive component centered at the frequency of the carrier modulated by the MLS. In order to produce a watermark at the maximal level, the amplitude is chosen equal to the local energy.

3.2.2 Edges and Textures Discrimination

Nevertheless, this simple implementation suffers from some drawbacks. Actually, the produced watermark is visible along contours and could be embedded with higher energy in the textured regions, i.e. in the regions that have a great activity.

The visibility problem brings some drawbacks of the perceptive model to the light. Because of their wideness (15 pixels), perceptive filters spread the peak of energy near sharp edges on a few pixels, leading to the embedding of the watermark in a rather large area around the edges. Particular studies about the masking phenomenon around sharp edges have shown that this phenomenon is strictly local, i.e. it concerns about three pixels around the edge [NH88]. A way to solve this problem is to make use of **edge detector filters**. These filters have good spatial localization, i.e. they permit to localize precisely sharp edges. The used edge detectors evaluate the envelope of the original signal filtered by a large bandwidth filter [VO89] in the way described in section 2.3, thus it can be considered as another kind of local energy. In one dimension, impulse response of the analytic representation of this filter is:

$$S + jA \tag{9}$$

$$\begin{array}{lccccc} with\ S = [0 & -0.93 & 1.86 & -0.93 & 0] \\ and\ A = [0.45 & -1.55 & 0 & 1.55 & -0.45] \end{array}$$

In two dimensions, the energy results from the square mean of the energy estimated in horizontal and vertical direction. Figure 3.2.2 presents the local energy produced by these edge detector filters. Nevertheless, such filters do not discriminate isolated edges from edges in active areas. This is why they are followed by a non linear **morphological filtering** [HSZ87]. A *closing* of the edges detector energy increases the energy level between neighboring edges but does not modify it in the surroundings of isolated edges. The *structurant element* size fixes what neighboring edges are. The resulting energy has strong values located on sharp edges and spread on active areas, i.e. areas having a strong edges density.

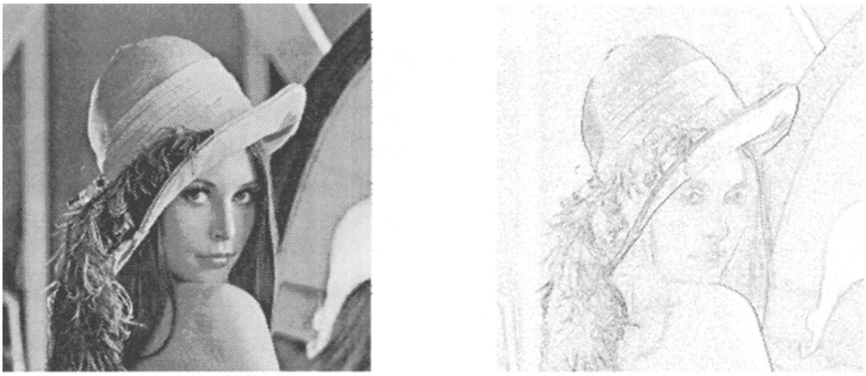

(a) (b)

Figure 3: Local energy from edge detector: (a) Lena Original (b) Lena filtered.

As a conclusion, the information produced through this edge detector and morphological filtering brings precise information about the location of the picture masking features. This permits to correct the result obtained from the perceptive filtering, which provides a direct information about the level of inscription allowed in the perceptive component of the carrier frequency but which suffers from weak localization capabilities. Actually, the MLS amplitude corresponds to the minimum of the perceptive energy and of twice the edge detectors energy value (it is worth noticing at this stage that both perceptive and edges detecting filters have been normalized, i.e. their maximal value in the frequency domain is equal to one). This correction procedure do not heavily increase the computational cost but permits to reduce the embedding near isolated edges. The resulting inscription scheme is illustrated on figure 3.2.2. The embedded bitstream contains some synchronization bits (see section 4.2.2). Some parts of this figure need further explanation. The inferior branch of the scheme evaluates the sign of the original picture contribution in the correlation computation. The sign of the embedded MLS is chosen to increase the absolute value of this contribution. The last band pass filter, coming before the addition of the watermark to the original picture, ensures that the embedded signal is really narrow band (see section 3.1.2). Finally, the limiter maintains pixels values between 0 and 255.

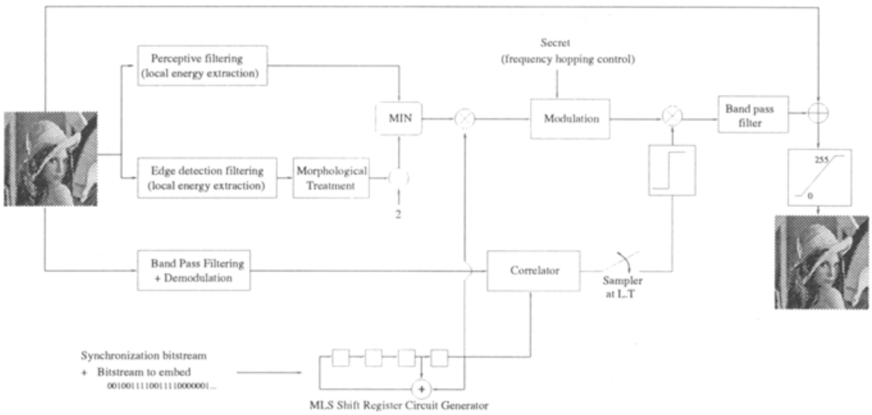

Figure 4: Watermark embedding procedure.

4 Results

4.1 Invisibility and Information Decoding Efficiency

When comparing the original and tha watermarked pictures, it is most of the time impossible to perceive a difference between them. Concerning the decoding efficacy, tests revealed that the MLS phase is misreceived in only a few cases (Figure 4.1(a)). Moreover, some a priori knowledge may help to predict error occurrence, since errors mainly occur in regions having a high ratio between energy variance and energy mean value(Figure 4.1(c)). An effective error detecting/correcting strategy has not yet been developed but this observation may be useful to locate the error when it has been detected, e.g. thanks to error detecting codes [Pur95]. Eventually, figure 4.1(b)represents the histogram of the rank of the embedded MLS reception in the decreasing ordered list of the reception values generated by all the shifted versions of the MLS. It shows that when an error occurs, i.e. there exists a shifted MLS giving a greater correlation value than the one obtained by correlating with the embedded MLS, the correct phase may be recovered by taking the phase of the sequence having the second correlation value.

4.2 System Robustness

4.2.1 JPEG

The embedded MLS is not removed by JPEG compression. Figure 4.2.1 shows the evolution of the correlation value with regards to the JPEG quality

Picture	Lena	Boat	Demi
Error rate (Misreceived sequences number)	1/33	1/33	4/33

(a)

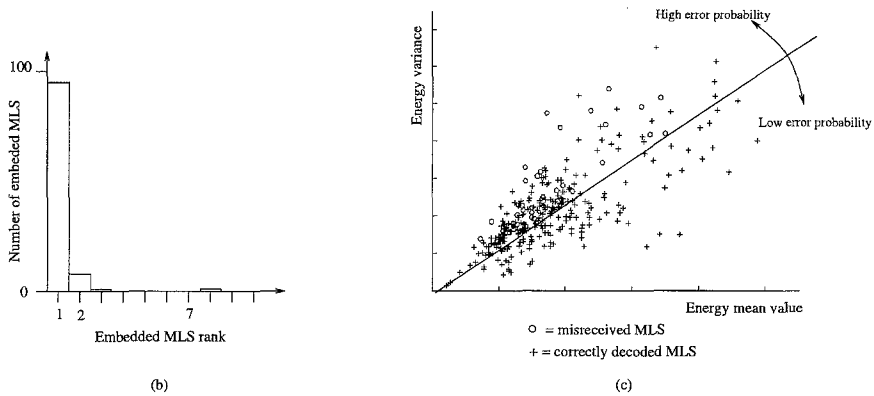

Figure 5: (a)Decoding error rate,(b)Phase detection histogram,(c)Variance/mean ratio.

percentage. The correlation has been normalized according to the value obtained at the reception of the non compressed watermarked picture.

4.2.2 Synchronization and Resistance Against Piracy

The synchronization is a major problem during the decoding, i.e. the acquisition of the MLS phase and of the carrier phase. Choosing to bind the carrier phase to the MLS phase reduces these problems to one synchronization. This problem has been omitted during the tests as the embedding always began at the first column of the digital picture. Nevertheless, in the context of analog video product watermarking, the digitization may be slightly different between the coding and the decoding. So, this problem is crucial in some applications. A possible approach to solve it would be to embed some known bits as a part of the watermark. These bits could be localized at the reception side through the search of a maximum of correlation along the received sequence. Once the synchronization is achieved, correlation properties of MLS could be used to compensate small shifting in the MLS phase, due for example to the loss of a column of the picture.

The parameters of the embedding procedure holds in the choice of the MLS and of the carrier frequency. Lets evaluate the number of possible choices for a 512x512 picture. About the MLS, there exists 186 31-ary MLS [Pet]. Concerning the carrier frequency, about hundred frequencies are available in the interval $[0.1, 0.2]$ of the normalized frequencies because, carriers having a $\Delta f_{normalized} \geq \frac{0.1}{100}$ can be considered as being orthogonal on the length of a MLS. Moreover for each embedded MLS, one can choose a different carrier. There are 33 embed-

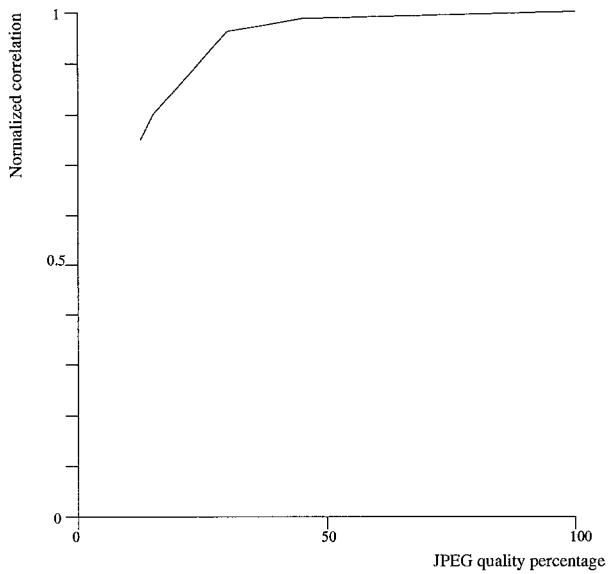

Figure 6: Correlation with regards to JPEG quality percentage.

ded MLS. There are thus 100^{33}, i.e. 2^{220} possibilities to choose the embedding parameters. This number is huge but does not represents the actual system robustness against a pirate because the analysis of the decoding correlations obtained by decoders tuned on 100 distinct frequencies and the 186 possible MLS may brought some information about the used parameters due to the appearance of particular peak features in the correlation. Nevertheless, due to his ignorance of the synchronization bits , the pirate is confronted with a strong phase acquisition problem: "How to choose the phase of the MLS carrier during the reception process?". It is noticeable that the very high noisy channel features prevents the pirate from using a classical *Phase Locking Loop.*

Due to the same reasons, it is of course possible to embed different watermarks. There exists 2^{220} possibilities to embed the watermark. However, as there are only 100 frequencies available, in average, one percent of the MLS will be modulated at the same frequency in the different watermarks, which entails 0.5 percent of wrong bits. This will not decrease significantly the robustness thanks to the use of error correcting codes.

5 Conclusion

The major interest of the proposed method is its low cost, since it has been designed to be implemented in real time and with rather low memory requirements. This is due to the fact that, during the watermarking process, only a few lines of the picture are considered. However, despite its simplicity, this method is also very efficient and resistant against JPEG compression. First results have shown that it permits to embed 165 bits in a picture of 512x512 pixels with an error rate lower than 10 percent in the worst cases. Moreover, first observations have shown that further investigations about the error occurrences should lead to a strong reduction of this error rate without reducing significantly the amount of information bits. Further studies will consider this topic and will also tackle the phase acquisition problem that is strongly related to the system robustness towards piracy.

References

[BGM95] W. Bender, D. Gruhl, and N. Moromoto. Techniques for data hiding. *Proceedings of the SPIE, san Jose*, 2420(40), February 1995.

[BQM95] O. Bruyndonckx, J.J. Quisquater, and B. Macq. Spatial method for copyright labelling of digital images. *Proceedings of IEEE Workshop on Non-Linear Processing, Thessaloniki*, pages 456–459, June 1995.

[BSLO94] J.T. Brassil, N.F. Maxemchuk S. Low, and L. O'Gorman. Electronic marking and identification techniques to discourage document copying. *Proceedings of IEEE INFOCOM'94, Toronto*, pages 1278–1287, June 1994.

[Car95] G. Caronni. Assuring ownership rights for digital images. *Proceeding of reliable IT systems, VIS 95, Germany*, June 1995.

[CKLS95] I.J. Cox, J. Kilian, T. Leighton, and T. Shamoon. Spread spectrum watermarking for multimedia. *Proceedings of the SPIE, San Jose*, 2420:456–459, February 1995.

[Com95] S. Comes. *Les traitements perceptifs d'images numérisées*. PhD thesis, Université catholique de Louvain, June 1995.

[DDVB96] J.F. Delaigle, C. De Vleeschouwer, and Macq B. Digital Watermarking. In *Conference 2659 - Optical Security and Counterfeit Deterrence Techniques*, San Jose, February 1996. SPIE Electronic Imaging: science and technology. pp. 99-110.

[HSZ87] R.M. Haralick, S.R. Sternberg, and X. Zhuang. Image Analysis Using Mathematical Morphology. *IEEE Transactions on Pattern Analysis and Machine Intelligence*, 9(4):532–550, July 1987.

[Kah94] B. Kahin. The Strategic Environment for Protecting Multimedia. *ima intellectual property project proceedings*, volume 1, pages 1–8, January 1994.

[KZ95] E. Koch and J. Zaho. Towards robust and hidden image copyright labeling. *Proceedings of IEEE Workshop on Non-Linear Processing, Thessaloniki*, pages 452–455, June 1995.

[MQ94] B. Macq and J.J. Quisquater. Digital images multiresolution encryption. *The journal of the Interactive Multimedia Association Intellectual Property Project*, 1:187–206, January 1994.

[MT94] K. Matsui and K. Tanaka. Video-stenography: How to embed a signature in a picture. *IMA Intellectual Property Proceedings*, 1(1):187–205, January 1994.

[NH88] A.N. Netraveli and B.G. Haskell. Visual Psychophysics. In *Digital Picture: Representation and Compression*, chapter 3. Plenum Press, New-York, 1988.

[Pet] Ray H. Pettit. Codes for Spread Spectrum. In *ECM and ECCM Techniques for Digital Communication Systems*, chapter 3, pages 37–60. Lifetime Learning Publications, Belmont California.

[Pur95] M. Purser. *Introduction to Error Correcting Codes.* Artech House, Boston-London, 1995. ISBN 0-89006-784-8.

[SM80] D.V. Sarwate and Pursley M.B. Crosscorrelation Properties of Pseudorandom and Related Sequences. *Proceedings of the IEEE*, 68(5):593–617, May 1980.

[VO89] S. Venkatesh and R. Owens. Implementation Details of a Feature Detection Algorithm. Technical Report 89/12, Department of Computer Science, University of Western Australia, 1989.

[WMP83] H.R. Wilson, D.K. McFarlane, and G.C. Phillips. Spatial Frequency Tuning of Orientation Selective Units Estimated by Oblique Masking. *Vision Research*, 23(9):873–847, 1983.

[WOT86] John Wiley, L.A. Olzak, and J.P. Thomas. *Handbook of perception and human performance. Volume 1: Sensory processes and perception. Chapter 7: Seeing spatial patterns.* University of California, Los Angeles, California, 1986.

[WP84] H.R. Wilson and G.C. Phillips. Orientation Bandwiths of Spatial Mechanisms Measured by Masking. *J. Opt. Soc. Am. A*, 1(2):226–232, February 1984.